Covalent EGFR inhibitor analysis reveals importance of reversible interactions to potency and mechanisms of drug resistance

Phillip A. Schwartz[a], Petr Kuzmic[b], James Solowiej[a], Simon Bergqvist[a], Ben Bolanos[c], Chau Almaden[a], Asako Nagata[c], Kevin Ryan[c], Junli Feng[c], Deepak Dalvie[d], John C. Kath[c], Meirong Xu[a], Revati Wani[a], and Brion William Murray[a,1]

[a]Oncology Research Unit, [c]Worldwide Medicinal Chemistry, and [d]Pharmacokinetics and Drug Metabolism, Pfizer Worldwide Research and Development, La Jolla, Pfizer Inc., San Diego, CA 92121; and [b]Research and Development, BioKin Ltd., Watertown, MA 02472

Edited* by Napoleone Ferrara, University of California, San Diego, La Jolla, CA, and approved November 25, 2013 (received for review July 23, 2013)

Covalent inhibition is a reemerging paradigm in kinase drug design, but the roles of inhibitor binding affinity and chemical reactivity in overall potency are not well-understood. To characterize the underlying molecular processes at a microscopic level and determine the appropriate kinetic constants, specialized experimental design and advanced numerical integration of differential equations are developed. Previously uncharacterized investigational covalent drugs reported here are shown to be extremely effective epidermal growth factor receptor (EGFR) inhibitors (k_{inact}/K_i in the range 10^5–10^7 $M^{-1}s^{-1}$), despite their low specific reactivity ($k_{inact} \leq 2.1 \times 10^{-3}$ s^{-1}), which is compensated for by high binding affinities ($K_i < 1$ nM). For inhibitors relying on reactivity to achieve potency, noncovalent enzyme–inhibitor complex partitioning between inhibitor dissociation and bond formation is central. Interestingly, reversible binding affinity of EGFR covalent inhibitors is highly correlated with antitumor cell potency. Furthermore, cellular potency for a subset of covalent inhibitors can be accounted for solely through reversible interactions. One reversible interaction is between EGFR-Cys_{797} nucleophile and the inhibitor's reactive group, which may also contribute to drug resistance. Because covalent inhibitors target a cysteine residue, the effects of its oxidation on enzyme catalysis and inhibitor pharmacology are characterized. Oxidation of the EGFR cysteine nucleophile does not alter catalysis but has widely varied effects on inhibitor potency depending on the EGFR context (e.g., oncogenic mutations), type of oxidation (sulfinylation or glutathiolation), and inhibitor architecture. These methods, parameters, and insights provide a rational framework for assessing and designing effective covalent inhibitors.

cysteine oxidation | protein kinase | signaling | capture period | warhead interactions

Receptor tyrosine kinases, such as the epidermal growth factor receptor (EGFR) tyrosine kinase, catalyze protein phosphorylation reactions to trigger signaling networks. Oncogenic activating mutations of EGFR lead to aberrant signaling for a subpopulation (10–30%) of nonsmall cell lung cancer patients (1). These mutations reside primarily in two regions of the EGFR catalytic domain [namely, the in-frame deletion mutations (e.g., Del746-750) preceding the N-terminal Cα-helix (exon 19) and the C-terminal activation loop L858R mutation (exon 21)] (2). Patients harboring these activating mutations usually respond to reversible ATP competitive drugs (e.g., erlotinib and gefitinib), but their effectiveness is limited by the emergence of drug resistance, in part, through an additional active site mutation (T790M and gatekeeper residue) in 50% of the responsive patients (3).

A second generation of drug discovery dating back to the 1990s resulted in inhibitors that incorporate a chemically reactive Michael Acceptor (MA) electrophile (warhead) to target a cysteine nucleophile (EGFR-Cys_{797}) in the hinge region of the ATP binding cleft (4). The ensuing 1,4-conjugate addition reaction of these inactivators results in an irreversible covalent adduct (Fig. 1*A*); hence, the term covalent inhibitors is used (5). To date, clinical trials of covalent EGFR inhibitors have produced mixed results (6, 7). The first covalent drug (CI-1033) did not proceed beyond early clinical studies. The next series of covalent inhibitors has advanced to phase III studies or are Food and Drug Administration-approved (3) [dacomitinib, PF-00299804 (8); neratinib, HKI-272 (9); afatinib, BIBW-2992 (10)]. Emerging clinical evidence indicates that these drugs can have superior clinical performance relative to reversible drugs but are also limited by the emergence of drug resistance (11, 12).

Covalent inhibition has reemerged as a protein kinase drug design strategy for a number of reasons (13, 14). The scope of the approach has recently expanded beyond the 11 EGFR-related kinases (e.g., HER2 and BTK) to 193 kinases that have a cysteine exposed in other regions of the active site (15). A subset of the covalent drugs is emerging as superior to reversible drugs (11, 12), which may be because of prolonged pharmacodynamic activity, lower dose, and more complete target inhibition (3). However, this mode of inhibition carries the risk of creating an immune response to epitopes from either expected or nonspecific covalent modifications (16). Therefore, the clinical benefit can outweigh the risks for well-designed inhibitors that maximize the benefit of reactivity and minimize its liability. To date, the distinct and separate contributions of noncovalent binding affinity and chemical reactivity to overall potency for the covalent EGFR investigational drugs have not been defined (17).

Significance

Covalent kinase inhibition strategies are reemerging, but critical gaps in the understanding of molecular determinants of potency still persist. A kinetic approach is developed to describe the components of overall inhibitor potency (reversible binding and chemical reactivity). Detailed kinetic descriptions of EGFR covalent drugs are provided. Reversible interactions of covalent inhibitors are found to be essential to biochemical and cellular potency. A dynamic linkage between available affinity and necessary reactivity is proposed. Cysteine oxidation is an emerging type of posttranslational modification. Specific oxidation of the EGF receptor cysteine nucleophile causes highly variable effects on inhibitor potency. Two mechanisms of drug resistance are identified (reversible cysteine–inhibitor warhead interactions and specific cysteine oxidation) as well as a rational framework for understanding and designing covalent inhibitors.

Author contributions: P.A.S., J.S., S.B., A.N., and B.W.M. designed research; P.A.S., J.S., S.B., B.B., C.A., A.N., K.R., J.F., D.D., and M.X. performed research; P.K. and J.C.K. contributed new reagents/analytic tools; P.A.S., P.K., S.B., B.B., A.N., R.W., and B.W.M. analyzed data; and B.W.M. wrote the paper.

Conflict of interest statement: All authors are employed by the companies designated in the affiliations.

*This Direct Submission article had a prearranged editor.

Freely available online through the PNAS open access option.

[1]To whom correspondence should be addressed. E-mail: brion.murray@pfizer.com.

This article contains supporting information online at www.pnas.org/lookup/suppl/doi:10.1073/pnas.1313733111/-/DCSupplemental.

BIOCHEMISTRY

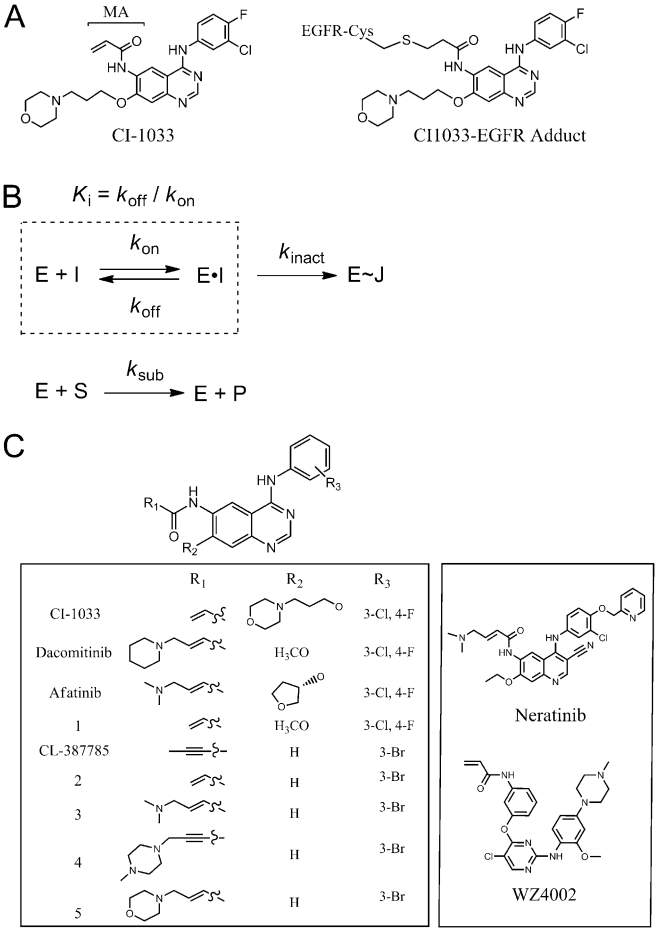

Fig. 1. (*A*) Chemical mechanisms of irreversible enzyme inhibition. Representative covalent inhibitor with reactive MA (bracket) and the resulting EGFR adduct. (*B*) The postulated kinetic mechanism for two-step covalent inhibition under the special experimental conditions where the Michaelis constant for the peptide substrate, S, is very much lower than the corresponding Michaelis constant $K_{m,Pep}$. The dashed box represents the rapid equilibrium approximation for inhibitor binding and dissociation. (*C*) Structures of EGFR covalent inhibitors investigated in this report.

In biochemical assessments of these highly potent drugs, the kinetic analysis is difficult, because deriving an exact algebraic solution is "hopelessly complex" (18). Nonetheless, defining the components of covalent inhibitor potency is important, because unlike other enzyme classes (e.g., proteases), the deep kinase active site cleft facilitates high-affinity inhibitor binding; thus, chemical reactivity can be rationally incorporated.

There is a growing appreciation that oxidation of cysteine residues affects signaling networks (19–21), including a report that EGFR is oxidized by hydrogen peroxide (H_2O_2) at Cys_{797} (the reactive nucleophile) (22, 23). Because oxidation fundamentally affects the chemical properties of the cysteine thiol by transforming it to either a highly polar oxo-acid or a bulky glutathione adduct, the EGFR active site topography and conformation may be affected. Therefore, oxidation of the nucleophilic Cys_{797} thiol has the potential to alter catalytic properties as well as covalent inhibitor potency and possibly, drug resistance. Taken together, the components of covalent inhibitor potency are critical to understanding biological effects as well as facilitating rational drug design.

Results

Defining the Covalent and Noncovalent Contributions to Overall Inhibitor Potency. The concentration of EGFR peptide substrate $[Pep]_0$ is very much lower than the corresponding Michaelis constant $K_{m,Pep}$, which makes it necessary to invoke a truncated hit-and-run (E + S → E + P) mechanistic model (Fig. 1*B* and *SI Appendix*, sections 1.1 and 1.2 show the derivation). If the peptide solubility was not a limitation, other kinetic regimes would be possible. The corresponding mathematical formalism as a system of simultaneous first-order ordinary differential equations is derived in *SI Appendix*, Section 3. The noncovalent K_i values are determined by two independent methods. The first method is based on the initial reaction rates analyzed by an algebraic fitting model (*SI Appendix*, section 2 and Table S1). This method relies on the fact that the initial enzyme–inhibitor complex is formed instantaneously on the timescale of the experiment. This rapid equilibrium assumption is applicable for all EGFR inhibitors investigated, because the empirically determined initial rates vary strongly with the inhibitor concentration, and this variation of initial rates follows the Morrison equation (24) for tight binding inhibition (*SI Appendix*, section 2, Fig. S6, and Table S1). A second, independent method of kinetic analysis relies on the global fit of complete reaction progress curves using a suitable differential equation numerical integration fitting model (*SI Appendix*, section 3). The two sets of noncovalent K_i values, determined by two independent methods, showed very good agreement ($R^2 = 0.99$) (*SI Appendix*, section 3). The inactivation rate constant k_{inact} (Fig. 1*B*) is also determined by numerical integration approach. Thus, we separate the overall inhibitory effect into two contributing components: the strength of noncovalent binding and the chemical reactivity of the initial enzyme–inhibitor complex.

Biochemical Kinetic Benchmarking of Covalent Inhibitors to WT EGFR. With this kinetic system, the first complete kinetic description of covalent drug potencies to their original therapeutic target (WT) is now possible (Fig. 2 and Table 1). Overall, the quinazoline-based covalent drugs (dacomitinib, afatinib, and CI-1033) are extremely effective ($k_{inact}/K_i = 6.3–23 \times 10^6$ $M^{-1}s^{-1}$) with high affinity ($K_i = 0.093–0.16$ nM) and low specific reactivity ($k_{inact} \leq 2.1$ ms^{-1}). As expected, these drugs are potent inhibitors of WT EGFR autophosphorylation in A549 tumor cells ($IC_{50} = 2–12$ nM). The quinolone-based investigational drug neratinib has the identical reactive substituent as afatinib, but its affinity is 50-fold weaker, with 25-fold weaker overall biochemical potency (k_{inact}/K_i). The pyrimidine-based inhibitor WZ4002 has the same reactive substituent as CI-1033 with fivefold more intrinsic chemical reactivity; however, it has 260-fold less biochemical potency. From this analysis, covalent drugs can be extremely effective

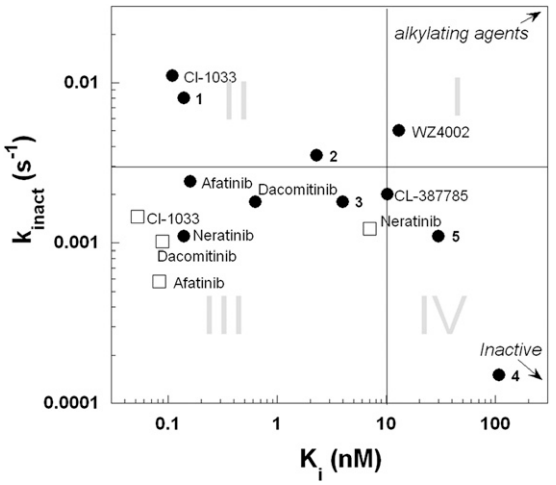

Fig. 2. Covalent drugs and inhibitors characterization based on kinetic properties with WT (□) and L858R/T790M EGFR (●): quadrant I, low affinity and high reactivity; quadrant II, high affinity and high reactivity; quandrant III, high affinity and moderate reactivity; quadrant IV, weak affinity and moderate to low reactivity.

Table 1. Kinetic analysis of covalent inhibition of EGFR-L858R/T790M WT EGFR

		EGFR-L858R/T790M				WT EGFR			
Inhibitor	GSH	K_i (nM)	k_{inact} (ms^{-1})	k_{inact}/K_i ($\mu M^{-1}s^{-1}$)	H1975 IC_{50} (nM)	K_i (nM)	k_{inact} (ms^{-1})	k_{inact}/K_i ($\mu M^{-1}s^{-1}$)	A549 IC_{50} (nM)
CI-1033	1.0	0.11 ± 0.03	11.0 ± 0.2	100 ± 20	2.3 ± 0.5	0.093 ± 0.002	2.9 ± 1.9	23 ± 1	4.9 ± 0.4
Dacomitinib	1.7	0.63 ± 0.05	1.8 ± 0.1	2.8 ± 0.3	10.3 ± 1.1	0.16 ± 0.01	1.5 ± 0.1	9.9 ± 0.8	2.5 ± 0.1
Afatinib	1.4	0.16 ± 0.03	2.4 ± 0.3	15 ± 4	7.3 ± 1.1	0.15 ± 0.01	0.9 ± 0.1	6.3 ± 0.8	11.5 ± 2.4
Neratinib	1.7	0.14 ± 0.03	1.1 ± 0.2	7 ± 2	9.4 ± 4.0	7.1 ± 0.4	1.8 ± 0.1	0.25 ± 0.01	5.2 ± 0.9
1	1.3	0.14 ± 0.07	8 ± 4	60 ± 40	6.6 ± 0.2	0.18 ± 0.01	2.3 ± 0.2	13 ± 1	5.8 ± 2.5
WZ-4002	4.8	13 ± 3	5.0 ± 0.1	0.40 ± 0.10	75 ± 25	28 ± 1	2.0 ± 0.1	0.089 ± 0.005	1,400 ± 400
CL-387785	5.0	10 ± 2	2.0 ± 0.3	0.21 ± 0.10	100 ± 7				
2	1.9	2.3 ± 0.3	3.5 ± 0.6	1.5 ± 0.3	30 ± 2				
3	2.2	4.0 ± 1.0	1.8 ± 0.1	0.40 ± 0.10	210 ± 3				
4	ND	108 ± 20	1.5 ± 0.2	0.0014 ± 0.0003	6,200 ± 3,200				
5	12.4	30 ± 3	1.1 ± 0. 1	0.04 ± 0.01	850 ± 90				

Intrinsic chemical reactivity is assessed by the reactivity to GSH relative to CI-1033 (CI-1033 half-life/inhibitor half-life). Cellular potency is quantitated by inhibition of EGFR-L858R/T790M autophosphorylation in H1975 tumor cells and EGFR WT in A549 tumor cells. ND, not determined.

EGFR inhibitors, but properties other than intrinsic chemical reactivity are critical to overall potency.

Biochemical and Cellular Characterization of Covalent Inhibition of Oncogenic EGFR. To better define the molecular determinants contributing to drug resistance as well as facilitate rational drug design of unique covalent inhibitors, the double mutant EGFR-L858R/T790M is profiled with a panel of covalent inhibitors (Table 1) encompassing three molecular scaffolds, two MAs, and the original EGFR covalent inhibitor series (3-bromo-anilino-quinazoline; CL-387785; **2**–**5**) (Fig. 1*C*) (25). Molecular modeling studies provide insight into the mode of binding for selected inhibitors (*SI Appendix*, Fig. S14). Although the quinazoline-based inhibitor **1** (PF-6274484) and the pyrimidine-based inhibitor WZ4002 share a common MA, the inhibitor scaffold places it in distinct orientations to Cys_{797}. For compound **1**, the nitrogen on the quinazoline ring interacts with the hinge region similar to EGFR drugs (gefitinib, lapatinib, and erlotinib), positioning the MA β-carbon 6 Å from Cys_{797}. WZ4002 binds to the hinge with the nitrogen on the pyrimidine ring, whereas the NH and phenoxy linkers position the MA β-carbon 3 Å from Cys_{797}. Chemical reactivity of the covalent inhibitors to the glutathione (GSH) thiol is used to assess nonenzymatic, intrinsic reactivity of these compounds (Table 1). Thus, the panel of covalent inhibitors covers a range of chemical properties and binding interactions.

Because covalent bond formation is thought to be critical, we explored the contribution of chemical reactivity to overall potency. The nonenzymatic reactivity to GSH varies only 12-fold across the inhibitor panel, whereas the specific enzymatic reactivity (k_{inact}) varies 73-fold (Table 1). There is no significant correlation between intrinsic GSH reactivity and k_{inact} ($R^2 = 0.13$), which is consistent with the EGFR architecture optimizing the reaction. There is only a moderate correlation of k_{inact} with inhibition of EGFR-L858R/T790M autophosphorylation in H1975 tumor cells ($R^2 = 0.60$) (*SI Appendix*, Fig. S10, circles). In contrast, the covalent inhibitor binding affinities (K_i) vary 750-fold across the panel (Table 1). Reversible binding affinity (K_i) correlates more strongly with cellular potency ($R^2 = 0.89$) (*SI Appendix*, Fig. S10, triangles). Overall biochemical potency as measured by the k_{inact}/K_i ratio is mostly strongly correlated with cellular potency ($R^2 = 0.95$) (*SI Appendix*, Fig. S10, squares). A broader analysis of 154 chemically diverse, cell-permeable covalent inhibitors encompassing six distinct core structures also shows a strong correlation of binding affinity with cellular potency (*SI Appendix*, Fig. S11). Inhibitor affinities are also determined for the oncogenic mutant EGFR-L858R (*SI Appendix*, Table S5). The quinazoline-based covalent drugs are found to have high binding affinities for EGFR-L858R ($K_i = 0.4$–0.7 nM), whereas the binding of pyrimidine-based WZ4002 is significantly weaker ($K_i = 13$ nM). Again, noncovalent binding affinities to EGFR-L858R are well-correlated with inhibiting EGFR-L858R autophosphorylation in tumor cells (H3255). We conclude that the initial noncovalent binding interactions leading to the formation of the initial enzyme–inhibitor complex make critically important contributions to cellular potency.

Nonreactive Analogs Reveal MA Contribution to Reversible Affinity. Nonreactive analogs of covalent inhibitors provide insight into the initial noncovalent interactions of covalent inhibitors, because the analogs have identical binding interactions, except for the fact that the MA has been fully reduced to an amide moiety (*SI Appendix*, Fig. S17). Surface plasmon resonance is used to measure the association and dissociation rate constants as well as the equilibrium binding constants of the reversible analogs of CI-1033 (**7**), dacomitinib (**8**), compound **1** (**9**), and WZ4002 (WZ4003) (*SI Appendix*, Tables S7 and S8). The dissociation equilibrium constants K_d for reversible analogs are compared with the biochemical inhibition constants K_i for the corresponding irreversible compounds. In all cases, the reversible (reduced) analogs seem to bind significantly more weakly compared with their reactive counterparts. In the case of WT EGFR, the smallest difference ($K_d/K_i = 5$) is seen for compound **7** vs. CI-1033, whereas the largest difference ($K_d/K_i = 22$) is seen for WZ4003 vs. WZ4002. The remaining two pairs of analogs in *SI Appendix*, Table S7 differ approximately by an order of magnitude ($K_d/K_i = 10$). These differences are more pronounced with EGFR-L858R/T790M, where the K_d/K_i ratio ranges from 24 (WZ4003 vs. WZ4002) to 420 (compounds **9** vs. **1**). The biochemical K_i values for the nonreactive analogs are in good agreement with their biophysical dissociation constant K_d. These results show that the MA moiety contributes significantly to the noncovalent binding affinity. The contribution of the MA to affinity is confirmed by results of cell-based assays (*SI Appendix*, Tables S5 and S6). The nonreactive analogs were evaluated to full-length, endogenous EGFR autophosphorylation in tumor cells. For example, the IC_{50} for the double mutant EGFR-L858R/T790M autophosphorylation inhibition in H1975 cells was 2.3 nM for CI-1033 but 1,800 nM (an 800-fold difference) for the corresponding nonreactive analog (compound **7**). Even more dramatically, whereas WZ4002 exhibited ~80 nM cellular IC_{50} in inhibiting both double mutant (EGFR-L858R/T790M) and single mutant (EGFR-L858R) autophosphorylation, the corresponding nonreactive analog is entirely inactive in cell-based assays. In contrast, nonreactive analogs of CI-1033 (**7**) and dacomitinib (**8**) are potent inhibitors of WT EGFR in A549 tumor cells: $IC_{50} = 16 \pm 2$ nM (**7**) and $IC_{50} = 13$ nM (**8**). The afatinib analog **6** has similar H3255 tumor cell potency (less than threefold difference compared with afatinib). Therefore, reversible MA interactions are highly variable and can contribute significantly to not only biochemical binding affinity but also, cellular potency.

Oxidation of EGFR-Cys_{797} Differentially Affects Catalysis and Inhibitor Potency. The effect of specific cysteine oxidation on inhibitor pharmacology has not been sufficiently described in the literature.

EGFR-L858R and EGFR-L858R/T790M proteins are selectively oxidized with either H_2O_2 or oxidized glutathione. Intact mass analysis reveals that a single mass shift occurs, which is consistent with either sulfinylation (-SO_2H) or S-glutathiolation. Tandem MS analysis encompassing all oxidizable residues (cysteine and methionine; 97% overall amino acid coverage) confirms that oxidation occurs exclusively at Cys_{797} (*SI Appendix*, Figs. S12 and S13). The resulting oxidized proteins are highly active, with no major change in catalytic parameters K_m and k_{cat} (*SI Appendix*, Table S4). These reagents enable us to investigate inhibitor interactions with specifically oxidized EGFR-Cys_{797}. Inhibitor binding affinities for specifically S-glutathiolated or sulfinylated EGFR-Cys_{797} are determined and compared with corresponding unoxidized forms (Fig. 3, Table 1, and *SI Appendix*, Tables S5 and S6). S-glutathiolation has the smallest effect on the reversible quinazoline drugs: 3- to 31-fold weaker affinity for EGFR-L858R (Fig. 3*A*) and 2- to 19-fold weaker affinity for EGFR-L858R/T790M (Fig. 3*B*). Quinazoline covalent inhibitors have moderately less affinity to S-glutathiolated EGFR-L858R (11- to 30-fold) (Fig. 3*C*), with much weaker affinity for S-glutathiolated EGFR-L858R/T790M (80- to 260-fold) (Fig. 3*D*). The pyrimidine inhibitor WZ4002 is a weak inhibitor of S-glutathiolated EGFR proteins (K_i > 1 μM; 170- to 400-fold less affinity) (Fig. 3*C*). EGFR-Cys_{797} sulfinylation has a distinct pharmacological profile relative to S-glutathiolation. The pyrimidine-based WZ4002 affinity is highly affected by sulfinylation of EGFR-L858R (1,100-fold) (Fig. 3*C*) and EGFR-L858R/T790M (110-fold) (Fig. 3*D*), resulting in ineffective inhibition (K_i = 1–10 μM). EGFR-L858R sulfinylation reduces reversible affinities of covalent drugs modestly (up to 12-fold) (Fig. 3*C*). Larger effects for sulfinylated EGFR-L858R/T790M (3- to 100-fold) (Fig. 3*D*) are observed when the affinity loss correlates with the complexity of the MA structure. For example, undecorated MAs (CI-1033, **1**, and WZ4002) have large affinity losses (110- to 390-fold), whereas those inhibitors with elaborate MAs (dacomitinib and afatinib) are less affected (4- to 13-fold). Taken together, the types of EGFR-Cys_{797} oxidation and inhibitor structure can profoundly alter inhibitor affinity to specifically oxidized EGFR.

Discussion

An impediment to understanding covalent drug potency is the use of overly simplified inhibitor analysis (e.g., IC_{50}) or incorrect kinetic analysis, which obscures the distinct molecular determinants (i.e., noncovalent binding affinity and chemical reactivity) that contribute separately to the overall inhibitor potency to the protein target (3, 26). In this work, we address this gap by taking a two-pronged approach. First, we optimized the experimental conditions to overcome the peptide insolubility limitation using hit-and-run experimental conditions (peptide substrate concentration very much lower than $K_{m,Pep}$ to simplify the interpretation of data and the ATP concentration very much higher than $K_{m,ATP}$ to increase assay sensitivity). Second, we introduce an advanced method of irreversible inactivation data analysis based on the numerical integration of the full system of simultaneous first-order ordinary differential equations (27). This approach allows us to efficiently define overall inhibitor potency in terms of contributions from reversible and irreversible components.

Having defined the individual determinants of inhibitory potency, we are able to organize covalent inhibitor potency space into four quadrants based on initial binding affinity and chemical reactivity (Fig. 2). Quadrant 1 contains alkylating agents that rely on intrinsic reactivity to achieve potency. Quadrant 4 is reserved for low-potency inhibitors. The challenge has been to discriminate between effective inhibitors that achieve potency by high affinity and reactivity (quadrant 2) or high affinity and moderate reactivity (quadrant 3). Covalent EGFR drugs have extremely high affinity and low reactivity to WT EGFR (quadrant 3). However, for EGFR-L858R/T790M, afatinib and CI-1033 map to quadrant 2, which indicates that the drug-resistant form of EGFR presents Cys_{797} differently.

The individual kinetic parameters can be used to characterize the molecular interactions underlying overall inhibitory potency. The K_i value is relatively simple to interpret, because it measures reversible binding affinity. In contrast, many different factors influence the k_{inact} value, including intrinsic chemical reactivity, reactant alignment, enforced local concentration, and the cysteine pK_a. To enhance the use of the microscopic rate constant k_{inact}, we introduce its inverse value ($1/k_{inact}$) and assign to it the term capture period (t_C) measured in the units of time. The typical values of k_{inact} for EGFR inhibitors in this study ranged from 1 to 10 ms^{-1}, which corresponds to t_C = 1,000 s (~15 min) and t_C = 100 s (~1.5 min), respectively. The capture period concept is analogous to the notion of reversible inhibitor residence time ($1/k_{off}$) (17), which has found use in drug design. These two values can be used in concert to facilitate rational covalent inhibitor design.

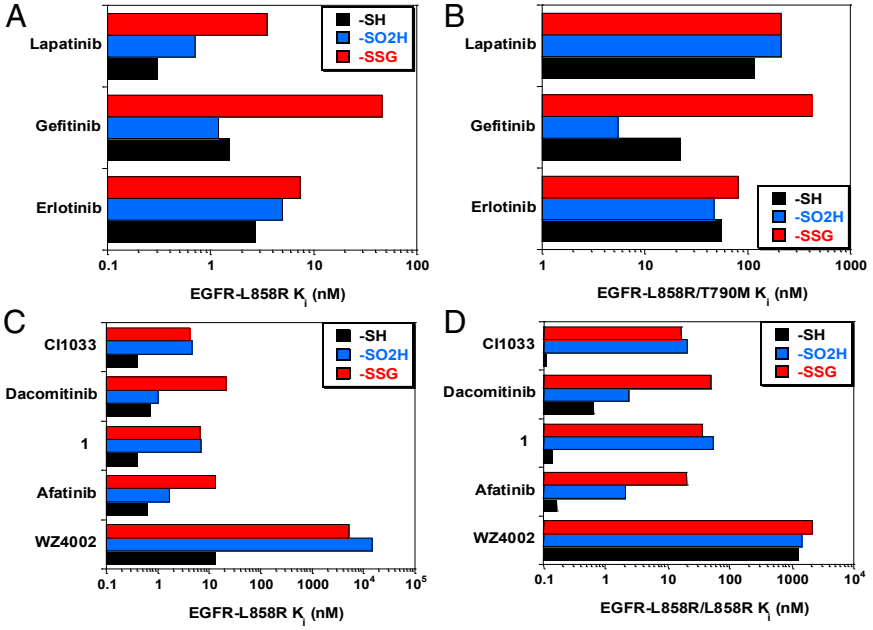

Fig. 3. Specific EGFR-Cys_{797} oxidation has differential effects on inhibitor and drug potencies dependent on the type of oxidation and EGFR mutation. Reversible drug affinity determined to different Cys_{797} oxidation states (-SH, unoxidized; -SO_2H, sulfinylated; -SSG, glutathiolated) in (*A*) L858R and (*B*) L858R/T790M. Covalent inhibitor affinity was measured to (*C*) L858R and (*D*) L858R/T790M.

Reversible EGFR Complexes with Covalent Inhibitors Are Integral to Overall Potency. The contribution of a reversible enzyme–inhibitor complex to covalent inhibitor potency is currently underappreciated. For example, covalent EGFR inhibitors have been incorrectly reported to have an infinite active site residence time (28), implying that the inhibitor never actually dissociates from the initially formed noncovalent complex. However, our analysis shows that the reversible inhibitor–EGFR complex preceding the covalent adduct formation is critical to cellular potency. Reversible inhibitor binding to EGFR affects the chemical reaction by multiple mechanisms. First, it defines the MA moiety orientation to the cysteine nucleophile. Second, it increases the effective reactant concentrations. Third, it defines the number of binding/release cycles necessary for a chemical reaction to occur. Nonproductive binding events (no reaction) should be expected for many reasons, such as misaligned reactants (protein conformations are dynamic) or cysteine nucleophile in the less-reactive thiol form. An important aspect of the reversible inhibitor complex typically overlooked is that it alone is sufficient to block enzymatic function.

MA Contributes a Key Reversible Interaction to Binding Affinity. Covalent inhibitor complexes that do not result in adduct formation may still have reversible Cys_{797}•MA interactions that can contribute to potency. Binding affinity of all covalent inhibitors can now be directly measured by enzyme kinetics to quantify the sum of all binding interactions. Nonreactive analogs have identical structures, except that they do not have the rigid, planar, π-electron–containing MA substituent. Therefore, the difference in covalent inhibitor and reversible analog affinities could result from reversible Cys_{797}•MA interactions. Although the difference in affinities could be caused by steric interactions of the flexible, nonreactive substituent, it is probably a minor component, because the nonreactive quinazoline inhibitors have EGFR-L858R affinities similar to covalent inhibitors. A precedent for S–π or SH–π interactions is found in both model systems (e.g., H_2S–benzene) (29) and protein structures (30) with the capability of contributing significant binding energy (e.g., 2.6 kcal/mol). We find that the contribution of the reversible Cys_{797}•MA interactions to potency can be large and depend on both inhibitor properties and EGFR context. Therefore, covalent inhibitor affinity can be derived, in part, by reversible MA interactions with EGFR-Cys_{797}.

Expression of Covalent Inhibitor Potency in Tumor Cells. We have shown that overall covalent inhibitor biochemical potency is derived from contributions of reversible binding affinity and covalent adduct formation. Cellular analysis of covalent inhibitors is complicated, because as they achieve higher affinity, the need for covalent adduct formation becomes less important. Contributing to the complexity is that in cells, protein kinases are subject to temporal regulation by multiple cellular mechanisms (e.g., activation, trafficking, recycling, and degradation) (31, 32). The translation of biochemical interactions to cellular potency can now be more finely dissected with the array of tools available. Quinazoline covalent inhibitors have extremely high reversible affinity. Nonreactive analogs of CI-1033 and dacomitinib are still very effective inhibitors of WT ($K_d \sim 1$ nM, A549 $IC_{50} \sim 10$ nM). Although the covalent adduct formation does occur, the expression of cellular potency can be accounted for solely by reversible interactions, which include those interactions with the MA. The cellular potency gained through the inclusion of a reactive MA correlates with the enhanced reversible affinity of the covalent inhibitor. In the context of L858R/T790M mutations, there is significantly less affinity for the reversible analogs of dacomitinib and CI-1033 (K_d = 20–50 nM), and thus, the MA contributes to reversible affinity by 30- to 400-fold. In contrast, other inhibitors may rely more heavily on covalent adduct formation to achieve potent inhibition. The pyrimidine inhibitor WZ4002 has a different Cys_{797}•MA orientation (*SI Appendix*, Fig. S14). and without a reactive MA, there is no detectable cellular potency. Collectively, understanding the contribution of reversible binding interactions is critical to defining the molecular interactions resulting in cellular potency.

Potential Mechanisms of Covalent Inhibitor Drug Resistance. The more fine-grained characterization of covalent inhibitor properties made possible by our approach (examining k_{inact} and K_i separately) may explain conflicting reports on covalent drug resistance. One study reports that CI-1033 elicits a C797S resistance mutation in a cellular model system and causes an ∼200-fold reduction in cellular potency (33). Another study reports that a related covalent inhibitor CL-387785 does not elicit a C797S resistance mutation in H1975 cells and causes only a fourfold loss of cellular potency (34). We find that disrupting the reversible Cys_{797}•MA interaction of CI-1033 by eliminating the acrylamide MA results in 250-fold weaker affinity for EGFR-L858R/T790M and an 800-fold reduction of cellular potency. This observation indicates a reliance of the reversible Cys_{797}•MA interaction, and CI-1033 drug resistance by C797S mutation seems likely. Replacement of the CL-387785 MA propyl alkynamide by a nonreactive methyl group results in only a 10-fold reduction in EGFR-L858R/T790M affinity ($K_i = 110 \pm 2$ nM), which predicts a lower reliance on a Cys_{797}•MA interaction and a lower likelihood of an additional C797S drug resistance mutation. Our analysis reinforces the concept that specific interactions of covalent inhibitors with EGFR-Cys_{797} are critical to the development of drug resistance.

Implications of Specific Oxidation of the Reactive Cysteine Nucleophile. Recently, the WT EGFR cysteine nucleophile EGFR-Cys_{797} was shown to be oxidized by H_2O_2 (22). However, the ultimate oxidation state was not elucidated, because a transient intermediate oxidation state was trapped (sulfenic acid and -SOH). We now show that the EGFR-Cys_{797} thiol can be stably oxidized to either the sulfinic acid ($-SO_2H$) or the S-glutathiolated adduct while retaining catalytic activity. Because EGFR-Cys_{797} is not expected to be an effective nucleophile when oxidized, the impact on covalent inhibition seems straightforward, because covalent bond formation is now precluded, which results in significant loss of overall effectiveness. However, covalent inhibitors can still undergo reversible association with the altered active site topography of oxidized EGFR. S-glutathiolation introduces substantial steric bulk, which can have both steric and conformational effects on inhibitor binding. H_2O_2 oxidation of the Cys_{797} thiol to sulfinic acid (Cys_{797}-SO_2H) introduces little additional steric bulk but substantially changes the residue's polarity. We identified certain effects of different oxidation states that are specific to a given inhibitor and the given EGFR mutant. Reversible EGFR-directed drugs, such as gefitinib, are not negatively affected by sulfinylation, whereas pyrimidine-based covalent inhibitors have low binding affinity under identical circumstances. Covalent quinazoline inhibitors display mixed effects, which may be caused by favorable sulfinylated cysteine residue interactions for those inhibitors with a well-aligned basic group substituent (dacomitinib, afatinib, and gefitinib) (*SI Appendix*, Figs. S15 and S16). From this biochemical analysis, the effect of cysteine oxidation can be highly variable depending on both the type of oxidation and specific inhibitor active site interactions.

Conclusions

A general approach is developed to characterize the component biochemical processes of covalent inhibitor potency. With this approach, we are able to determine both the equilibrium dissociation constant of the initial noncovalent complex and the chemical reactivity of the warhead moiety. Factoring the overall inhibitory effect into reversible and irreversible components enables a deeper understanding and description of this reemerging inhibition modality. Reversible interactions of covalent inhibitors with EGFR, including Cys_{797}•MA, are shown to be essential to both biochemical and cell potencies. In addition, specific cysteine oxidation has been identified here as a possible drug resistance mechanism. Taken together, we present a rational framework for understanding and optimizing covalent enzyme inhibitors, which encompasses the inhibitor structure, binding interactions, and the cysteine nucleophile.

Materials and Methods

Additional details are in *SI Appendix*.

Synthesis of Sulfinylated EGFR-Cys$_{797}$. EGFR-L858R (40 μM) or EGFR-L858R/T790M (40 μM) was incubated (15 min at 23 °C) in a 120-μL reaction [100 μM H_2O_2, 60 mM NaCl, 15 mM KCl, 0.01% Tween-20, 10% (vol/vol) glycerol, 100 mM $(NH_4)HCO_3$, pH 9.2] and loaded onto 3× Zeba spin desalting columns equilibrated with 150 mM NaCl, 10% glycerol, 0.01% Tween-20, and 2 mM DTT in 50 mM Hepes (pH 7.5) at 4 °C. Sulfinylation at Cys$_{797}$ was >90% by MS.

Synthesis of Glutathiolated EGFR-Cys$_{797}$. EGFR-L858R (8 μM) or EGFR-L858R/T790M (8 μM) was incubated for 185 min at 23 °C in a 600-μL reaction (2 mM oxidized glutathione, 100 mM NaCl, 0.01% Tween-20, 10% glycerol, 25 mM Hepes, pH 8.5). Reaction aliquots (0.20 mL) were concentrated fivefold (3× Microcon spin concentrators, 14,000 × *g* for 15 min at 23 °C) to 40 μL and loaded onto 3× Zeba spin desalting columns (100 mM NaCl, 10% glycerol, 0.01% Tween-20, 25 mM Hepes, pH 7.5) at 4 °C.

EGFR Kinase Activity Assays. A coupled enzymatic spectrometric assay measuring ADP production is used to determine catalytic constants and reversible inhibitor potency (35). Covalent inhibitor analysis uses an Omnia continuous fluorometric assay with a Y12 tyrosine phosphoacceptor peptide [Ac-EEEEYI(cSx)IV-NH_2; Invitrogen] (36).

Intrinsic Chemical Reactivity Assay. Inhibitor reactivity with GSH is assessed by monitoring inhibitor loss during the reaction: 0.1 M phosphate buffer (pH 7.4), 0.1 μM compounds, and 5 mM GSH at 37 °C. The intrinsic reactivity is reported as the ratio of half-lives: inhibitor to CI-1033 (CI-1033 $t_{1/2} = 10$ min).

EGFR Cellular Autophosphorylation ELISA. For tumor cell lines, inhibitors were incubated with cells (H3255, L858R; NCI-H1975, L858R/T790M; A549, WT) for 2 h. PathScan Phospho-EGF Receptor (Tyr1068) Sandwich ELISA (Cell Signaling Technology) was quantitated per the manufacturer's protocol.

Mass Spectrometric Analysis of EGFR. Intact mass analysis used electrospray ionization on an Agilent 6210 time-of-flight mass spectrometer coupled to an Agilent 1200 LC. To identify oxidized residues, a Proxeon nanoLC coupled to an LTQ mass spectrometer was used on samples isolated by nondenaturing PAGE, pepsin-proteolyzed, and purified by Reprosil ProteCol Trap C18-AQ and Halo ES-C18 columnchromatography. MS-MS data are processed in Agilent Spectrum Mill rev. 4.0.

Inhibitor Modeling and Docking Methodology. Simulations used Glide in Standard Precision mode. EGFR cocrystal structures [gefitinib, Protein Data Bank (PDB) ID code 2ITZ; lapatinib, PDB ID code 1XKK; erlotinib, PDB ID code 1M17] optimized and minimized for the docking simulation.

Analysis of Enzyme Kinetic Data. Initial reaction rates were determined by a least squares fit of the initial portion ($t_{max} < 7$ min) of progress curves to the single exponential equation. Dissociation constants of the initial noncovalent enzyme/inhibitor complex were determined by two independent methods: (*i*) from the initial reaction rates and (*ii*) from the global fit of the complete reaction progress curves. The underlying system of first-order ordinary differential equations was integrated using the LSODE algorithm (37–39).

ACKNOWLEDGMENTS. We thank Drs. Karen Maegley and Stephan Grant for helpful feedback. We also thank the Pfizer Postdoctoral Program for supporting the fellowships of P.A.S. and R.W.

1. Gazdar AF (2009) Activating and resistance mutations of EGFR in non-small-cell lung cancer: Role in clinical response to EGFR tyrosine kinase inhibitors. *Oncogene* 28(Suppl 1):S24–S31.
2. Sharma SV, Bell DW, Settleman J, Haber DA (2007) Epidermal growth factor receptor mutations in lung cancer. *Nat Rev Cancer* 7(3):169–181.
3. Schwartz PA, Murray BW (2011) Protein kinase biochemistry and drug discovery. *Bioorg Chem* 39(5–6):192–210.
4. Wissner A, Mansour TS (2008) The development of HKI-272 and related compounds for the treatment of cancer. *Arch Pharm (Weinheim)* 341(8):465–477.
5. Silverman RB (1995) Mechanism-based enzyme inactivators. *Methods Enzymol* 249: 240–283.
6. Jänne PA, et al. (2007) Multicenter, randomized, phase II trial of CI-1033, an irreversible pan-ERBB inhibitor, for previously treated advanced non small-cell lung cancer. *J Clin Oncol* 25(25):3936–3944.
7. Rixe O, et al. (2009) A randomized, phase II, dose-finding study of the pan-ErbB receptor tyrosine-kinase inhibitor CI-1033 in patients with pretreated metastatic breast cancer. *Cancer Chemother Pharmacol* 64(6):1139–1148.
8. Jänne PA, et al. (2011) Phase I dose-escalation study of the pan-HER inhibitor, PF299804, in patients with advanced malignant solid tumors. *Clin Cancer Res* 17(5):1131–1139.
9. Burstein HJ, et al. (2010) Neratinib, an irreversible ErbB receptor tyrosine kinase inhibitor, in patients with advanced ErbB2-positive breast cancer. *J Clin Oncol* 28(8):1301–1307.
10. Yang JC, et al. (2012) Afatinib for patients with lung adenocarcinoma and epidermal growth factor receptor mutations (LUX-Lung 2): A phase 2 trial. *Lancet Oncol* 13(5):539–548.
11. Kwak E (2011) The role of irreversible HER family inhibition in the treatment of patients with non-small cell lung cancer. *Oncologist* 16(11):1498–1507.
12. Singh J, et al. (2012) Superiority of a novel EGFR targeted covalent inhibitor over its reversible counterpart in overcoming drug resistance. *Med Chem Commun* 3:780–783.
13. Singh J, Petter RC, Baillie TA, Whitty A (2011) The resurgence of covalent drugs. *Nat Rev Drug Discov* 10(4):307–317.
14. Garuti L, Roberti M, Bottegoni G (2011) Irreversible protein kinase inhibitors. *Curr Med Chem* 18(20):2981–2994.
15. Leproult E, Barluenga S, Moras D, Wurtz JM, Winssinger N (2011) Cysteine mapping in conformationally distinct kinase nucleotide binding sites: Application to the design of selective covalent inhibitors. *J Med Chem* 54(5):1347–1355.
16. Nakayama S, et al. (2009) A zone classification system for risk assessment of idiosyncratic drug toxicity using daily dose and covalent binding. *Drug Metab Dispos* 37(9):1970–1977.
17. Copeland RA, Pompliano DL, Meek TD (2006) Drug-target residence time and its implications for lead optimization. *Nat Rev Drug Discov* 5(9):730–739.
18. Williams JW, Morrison JF, Duggleby RG (1979) Methotrexate, a high-affinity pseudosubstrate of dihydrofolate reductase. *Biochemistry* 18(12):2567–2573.
19. Paulsen CE, Carroll KS (2010) Orchestrating redox signaling networks through regulatory cysteine switches. *ACS Chem Biol* 5(1):47–62.
20. Poole LB, Nelson KJ (2008) Discovering mechanisms of signaling-mediated cysteine oxidation. *Curr Opin Chem Biol* 12(1):18–24.
21. Filosto S, et al. (2011) EGF receptor exposed to oxidative stress acquires abnormal phosphorylation and aberrant activated conformation that impairs canonical dimerization. *PLoS One* 6(8):e23240.
22. Paulsen CE, et al. (2012) Peroxide-dependent sulfenylation of the EGFR catalytic site enhances kinase activity. *Nat Chem Biol* 8(1):57–64.
23. Truong TH, Carroll KS (2012) Redox regulation of EGFR signaling through cysteine oxidation. *Biochemistry* 51:9954–9965.
24. Morrison JF (1969) Kinetics of the reversible inhibition of enzyme-catalysed reactions by tight-binding inhibitors. *Biochim Biophys Acta* 185(2):269–286.
25. Tsou HR, et al. (2001) 6-Substituted-4-(3-bromophenylamino)quinazolines as putative irreversible inhibitors of the epidermal growth factor receptor (EGFR) and human epidermal growth factor receptor (HER-2) tyrosine kinases with enhanced antitumor activity. *J Med Chem* 44(17):2719–2734.
26. Copeland RA (2005) *Evaluation of Enzyme Inhibitors in Drug Discovery* (Wiley, New York).
27. Szedlacsek SE, Duggleby RG (1995) Kinetics of slow and tight-binding inhibitors. *Methods Enzymol* 249:144–180.
28. Heuckmann JM, Rauh D, Thomas RK (2012) Epidermal growth factor receptor (EGFR) signaling and covalent EGFR inhibition in lung cancer. *J Clin Oncol* 30(27):3417–3420.
29. Ringer AL, Senenko A, Sherrill CD (2007) Models of S/pi interactions in protein structures: Comparison of the H2S benzene complex with PDB data. *Protein Sci* 16(10): 2216–2223.
30. Daeffler KN, Lester HA, Dougherty DA (2012) Functionally important aromatic-aromatic and sulfur-π interactions in the D2 dopamine receptor. *J Am Chem Soc* 134(36): 14890–14896.
31. Carpenter G, Liao HJ (2009) Trafficking of receptor tyrosine kinases to the nucleus. *Exp Cell Res* 315(9):1556–1566.
32. Murphy JE, Padilla BE, Hasdemir B, Cottrell GS, Bunnett NW (2009) Endosomes: A legitimate platform for the signaling train. *Proc Natl Acad Sci USA* 106(42): 17615–17622.
33. Avizienyte E, Ward RA, Garner AP (2008) Comparison of the EGFR resistance mutation profiles generated by EGFR-targeted tyrosine kinase inhibitors and the impact of drug combinations. *Biochem J* 415(2):197–206.
34. Yu Z, et al. (2007) Resistance to an irreversible epidermal growth factor receptor (EGFR) inhibitor in EGFR-mutant lung cancer reveals novel treatment strategies. *Cancer Res* 67(21):10417–10427.
35. Murray BW, Padrique ES, Pinko C, McTigue MA (2001) Mechanistic effects of autophosphorylation on receptor tyrosine kinase catalysis: Enzymatic characterization of Tie2 and phospho-Tie2. *Biochemistry* 40(34):10243–10253.
36. Luković E, González-Vera JA, Imperiali B (2008) Recognition-domain focused chemosensors: Versatile and efficient reporters of protein kinase activity. *J Am Chem Soc* 130(38):12821–12827.
37. Hindmarsh AC (1983) ODEPACK: A systematized collection of ODE solvers. *Scientific Computing*, ed Vichnevetsky R (North-Holland, Amsterdam), pp 55–64.
38. Kuzmic P (1996) Program DYNAFIT for the analysis of enzyme kinetic data: Application to HIV proteinase. *Anal Biochem* 237(2):260–273.
39. Kuzmic P (2009) DynaFit—a software package for enzymology. *Methods Enzymol* 467:247–280.